

4. PRODUCTION AND PROPERTIES OF RADIATIONS

4.2.3.5. Comments

For reliable experiments using XAFS and XANES to be undertaken, intense-radiation sources must be used. Synchrotron-radiation sources are such a source of highly intense X-rays. Their ready availability to experimenters and the comparative simplicity of the equipment required to perform the experiments have made experiments involving XAFS and XANES very much easier to perform than has hitherto been the case.

At some synchrotron-radiation sources, database and program libraries for the storage and analysis of XAFS and XANES data exist. These are usually part of the general computing facilities (Pantos, 1982).

Crystallographers seeking information concerning the nature and extent of these computer facilities can find such information by contacting the computer centre at one of the synchrotron-radiation establishments listed in Table 4.2.3.1.

4.2.4. X-ray absorption (or attenuation) coefficients (By D. C. Creagh and J. H. Hubbell)

4.2.4.1. Introduction

This data set is intended to supersede those data sets given in *International Tables for X-ray Crystallography*, Vols. III (Koch, MacGillavry & Milledge, 1962) and IV (Hubbell, McMaster, Del Grande & Mallett, 1974).

It is not intended here to give a detailed bibliography of experimental data that have been obtained in the past 90 years. This has been the subject of a number of publications, e.g. Saloman & Hubbell (1987), Hubbell, Gerstenberg & Saloman (1986), Saloman & Hubbell (1986), and Saloman, Hubbell & Scofield (1988). Further commentary on the validity and the quality of the experimental data in existing tabulations has been given by Creagh & Hubbell (1987) and Creagh (1987).

Existing tabulations of X-ray attenuation (or absorption) cross sections fall into three distinct categories: purely theoretical, purely experimental, and an evaluated mixture of theoretical and experimental data.

Compilations of the purely theoretically derived data exist for: photo-effect absorption cross sections (Storm & Israel, 1970; Cromer & Liberman, 1970; Scofield, 1973; Hubbell, Veigele, Briggs, Brown, Cromer & Howerton, 1975; Band, Kharitonov & Trzhaskovskaya, 1979; Yeh & Lindau, 1985);

Compton scattering cross sections (Hubbell *et al.*, 1975);

Rayleigh scattering cross sections (Hubbell *et al.*, 1975; Hubbell & Øverbø, 1979; Schaupp, Schumacher, Smend, Rullhausen & Hubbell, 1983).

Many purely experimental compilations exist, and the cross-section data given in computer programs used in the analysis of results in X-ray-fluorescence spectroscopy, electron-probe microanalysis, and X-ray diffraction are usually (evaluated) compilations of several of the following compilations: Allen (1935, 1969), Victoreen (1949), Liebhafsky, Pfeiffer, Winslow & Zemany (1960), Koch *et al.* (1962), Heinrich (1966), Theisen & Vollath (1967), Veigele (1973), Leroux & Thinh (1977), Montenegro, Baptista & Duarte (1978), and Plechaty, Cullen & Howerton (1981). If a comparison is made between these data sets, significant discrepancies are found, and questions must be asked concerning the reliability of the data sets that are compared. Jackson & Hawkes (1981) and Gerward (1986) have produced sets of parametric tables to simplify the application of X-ray attenuation data for the solution of problems in computer-aided tomography and X-ray-fluorescence analysis.

Compilations by Henke, Lee, Tanaka, Shimambukuro & Fujikawa (1982) and the earlier tables of McMaster, Del Grande, Mallett & Hubbell (1969/1970) are examples of the judicious application of both theoretical and experimental data to produce a comprehensive data set of X-ray interaction cross sections.

Because of the discrepancies that appear to exist between experimental data sets, the IUCr Commission on Crystallographic Apparatus set up a project to establish which, if any, of the existing methods for measuring X-ray interaction cross sections (X-ray attenuation coefficients) and which theoretical calculations could be considered to be the most reliable. A discussion of some of the major results of this project is given in Section 4.2.3. A more detailed description of this project has been given by Creagh & Hubbell (1987, 1990).

In this section, tabulations of the total X-ray interaction cross sections σ and the mass absorption coefficient μ_m are given for a range of characteristic X-ray wavelengths [Ti $K\alpha$ 2.7440 Å (or 4.509 keV) to Ag $K\beta$ 0.4470 Å (or 24.942 keV)]. The interaction cross sections are expressed in units of barns/atom (1 barn = 10^{-28} m²) whilst the mass absorption coefficient is given in cm² g⁻¹. Table 4.2.4.1 sets out the wavelengths of the characteristic wavelengths used in Tables 4.2.4.2 and 4.2.4.3, which list values of σ and μ_m , respectively.

Users of these tables should be aware of three important facts.

(i) The values given in the tables are derived for the case of isolated atoms, and cooperative effects may become important in condensed phases (Section 4.2.3).

(ii) The values are based solely on theoretical calculations.

(iii) The limits to the reliability of the data when compared with experimental values are shown in Fig. 4.2.4.4.

The linear attenuation coefficient μ_l in units of cm⁻¹ can be defined operationally as

$$\mu_l = \left(\ln \frac{I_0}{I} \right) / t \quad (4.2.4.1)$$

from the exponential attenuation relationship

$$\frac{I}{I_0} = \exp(-\mu_l t) \quad (4.2.4.2)$$

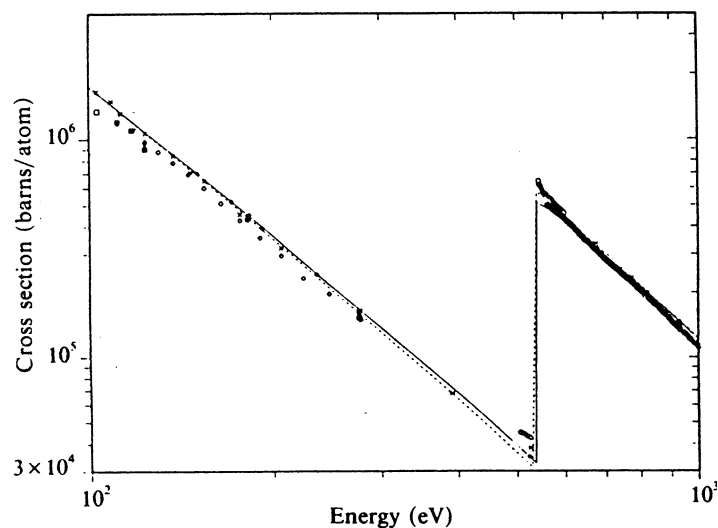


Fig. 4.2.4.1. Agreement between theory and experiment for oxygen ($Z = 8$) in the 'soft' X-ray region. The solid line is for the Scofield (1973) values without renormalization and the dotted line is for the semi-empirical data of Henke *et al.* (1982).

4.2. X-RAYS

Table 4.2.4.1. Table of wavelengths and energies for the characteristic radiations used in Tables 4.2.4.2 and 4.2.4.3

Radiation	λ (Å)	E (keV)
Ag $K\bar{\alpha}$	0.5608	22.103
$K\beta_1$	0.4970	24.942
Pd $K\bar{\alpha}$	0.5869	21.125
$K\beta_1$	0.5205	23.819
Rh $K\bar{\alpha}$	0.6147	20.169
$K\beta_1$	0.5456	22.724
Mo $K\bar{\alpha}$	0.7107	17.444
$K\beta_1$	0.6323	19.608
Zn $K\bar{\alpha}$	1.4364	8.631
$K\beta_1$	1.2952	9.572
Cu $K\bar{\alpha}$	1.5418	8.041
$K\beta_1$	1.3922	8.905
Ni $K\bar{\alpha}$	1.6591	7.472
$K\beta_1$	1.5001	8.265
Co $K\bar{\alpha}$	1.7905	6.925
$K\beta_1$	1.6208	7.629
Fe $K\bar{\alpha}$	1.9373	6.400
$K\beta_1$	1.7565	7.038
Mn $K\bar{\alpha}$	2.1031	5.895
$K\beta_1$	1.9102	6.490
Cr $K\bar{\alpha}$	2.2909	5.412
$K\beta_1$	2.0848	5.947
Ti $K\bar{\alpha}$	2.7496	4.509
$K\beta_1$	2.5138	4.932

in which an idealized plane-parallel slab of material is interposed normally into a parallel beam of monoenergetic X-rays initially of intensity I_0 , attenuated by the interposed slab to a reduced intensity I .

The linear attenuation coefficient μ_l for multi-element substances may be obtained in two ways. Through the mass absorption coefficients, we have

$$\mu_l = \rho \sum_i g_i (\mu_m)_i, \quad (4.2.4.3)$$

where g_i is the mass fraction of the element i for which the mass attenuation coefficient $(\mu_m)_i$ is in units of $\text{cm}^2 \text{g}^{-1}$, and ρ is the density of the material in units of g cm^{-3} . The summation is over all the constituent elements. The mass attenuation coefficient μ_m is sometimes written as (μ_l/ρ) .

For a crystal with unit-cell volume V_c ,

$$\mu_l = \frac{1}{V_c} \sum_i \sigma_i, \quad (4.2.4.4)$$

where the summation is over all the atoms in the cell. If σ_i is in barns/atom and V_c is in \AA^3 , then μ_l is in cm^{-1} .

These tables list total interaction cross sections and mass attenuation coefficients for isolated atoms calculated for characteristic X-ray photon emissions ranging from Ti $K\alpha$ to Ag $K\beta$.

The total interaction cross section is defined by

$$\sigma = \sigma_{pe} + \sigma_R + \sigma_C, \quad (4.2.4.5)$$

where σ_{pe} is the photo-effect cross section; σ_R is the Rayleigh (unmodified, elastic) cross section; σ_C is the Compton (modified, inelastic) cross section.

The reader's attention is drawn to the fact that in the neighbourhood of an absorption edge for aggregations of atoms significant deviations may be found because of cooperative effects (XAFS and XANES). A discussion of these effects is given in Section 4.2.3.

4.2.4.2. Sources of information

4.2.4.2.1. Theoretical photo-effect data: σ_{pe}

Of the many theoretical data sets in existence, those of Storm & Israel (1970), Cromer & Liberman (1970), and Scofield (1973) have often been used as bench marks against which both experimental and theoretical data have been compared. In particular, theoretical data produced using the S-matrix approach have been compared with these values. See, for example, Kissel, Roy & Pratt (1980). Some indication of the extent to which agreement exists between the different theoretical data sets is given in §4.2.6.2.4 (Tables 4.2.6.3 and 4.2.6.5). These tables show that the values of $f'(\omega, 0)$, which is proportional to σ , calculated using modern relativistic quantum mechanics, agree to better than 1%. It has also been demonstrated by Creagh & Hubbell (1987, 1990) in their analysis of the results of the IUCr X-ray Attenuation Project that there appears to be no rational basis for preferring one of these data sets over the other.

These tables do not list separately photo-effect cross sections. However, should these be required, the data can be found using Table 4.2.6.8. The cross section in barns/atom is related to $f'(\omega, 0)$ expressed in electrons/atom by $\sigma = 5636\lambda f'(\omega, 0)$, where λ is expressed in ångströms.

The values for σ_{pe} used in this compilation are derived from recent tabulations based on relativistic Hartree-Fock-Dirac-Slater calculations by Creagh. The extent to which this data set differs from other theoretical and experimental data sets has been discussed by Creagh (1990).

4.2.4.2.2. Theoretical Rayleigh scattering data: σ_R

If each of the atoms gives rise to scattering in which momentum but not energy changes occur, and if each of the atoms can be considered to scatter as if it were an isolated atom, the cross section may be written as

$$\sigma_R = \pi r_e^2 \int_{-1}^1 (1 + \cos^2 \varphi) f^2(q, Z) d(\cos \varphi), \quad (4.2.4.6)$$

where

r_e is the classical radius of the electron;

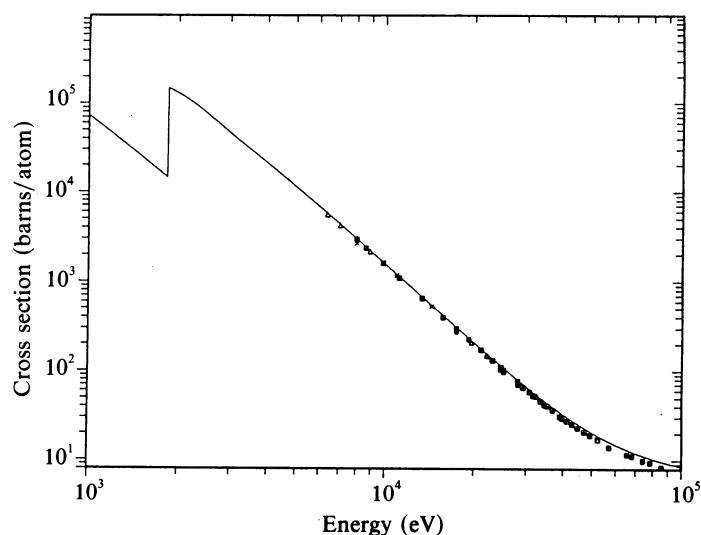


Fig. 4.2.4.2. The total cross section for silicon ($Z = 14$) compared with the unrenormalized Scofield values. The measured and theoretical attenuation coefficients show systematic differences of several percent for the photon energy range 10 to 100 keV.